JACS
JOURNAL OF THE AMERICAN CHEMICAL SOCIETY
Article
pubs.acs.org/JACS

Ultrathin and Ultralong Single-Crystal Platinum Nanowire Assemblies with Highly Stable Electrocatalytic Activity

Bao Yu Xia, Hao Bin Wu, Ya Yan, Xiong Wen (David) Lou,* and Xin Wang*

School of Chemical and Biomedical Engineering, Nanyang Technological University, 62 Nanyang Drive, Singapore 637459, Singapore

Supporting Information

ABSTRACT: Ultrathin one-dimensional (1D) nanostructures such as nanowires and nanorods have drawn considerable attention due to their promising applications in various fields. Despite the numerous reports on 1D nanostructures of noble metals, one-pot solution synthesis of Pt 1D nanostructures still remains a great challenge, probably because of the intrinsic isotropic crystal growth behavior of Pt. Herein, we demonstrate the facile solvothermal synthesis of nanowire assemblies composed of ultrathin (ca. 3 nm) and ultralong (up to 10 μm) Pt nanowires without involving any template. The oriented attachment mechanism is found to be partially responsible for the formation of such ultrathin Pt nanowires. The amine molecules generated during the reaction might assist the formation of nanowire assemblies. Importantly, the present system can be extended to synthesize Pt-based alloy nanowire assemblies such as Pt–Au and Pt–Pd. These Pt nanowires can be easily cast into a free-standing membrane, which exhibits excellent electrocatalytic activity and very high stability for formic acid and methanol oxidation and the oxygen reduction reaction.

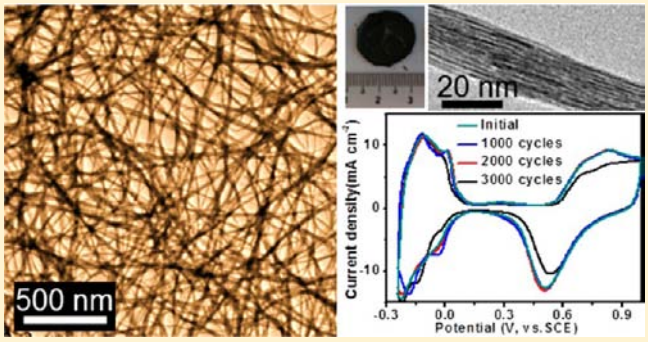

INTRODUCTION

Ultrathin noble-metal nanowires have attracted great attention for their unique photonic, electronic, magnetic, and catalytic properties.[1−7] Their synthesis has been realized by various approaches,[8−13] which mostly involve the use of templates or substrates,[14−19] such as biomaterials,[20−22] carbon nanotubes,[23] block copolymers,[24] and other mesoporous materials,[25] to guide the formation and growth of noble-metal nanowires. However, the subsequent requirement for template removal and the difficulty in scaling up limit their practical applications.[5] Ligand-assisted solution methods are effective for the synthesis of single-crystal noble-metal ultrathin nanowires.[26] For example, Xia's and Yang's groups have reported the oleylamine-assisted formation of ultrathin Au nanowires in solution.[27,28] Nonetheless, it generally remains a great challenge to directly synthesize ultrathin noble-metal nanowires without the use of templates or substrates. Another observation is that it is particularly difficult for platinum (Pt) to grow directly into one-dimensional (1D) single-crystal nanorods/nanowires with high aspect ratio in solution without the assistance of substrates or templates.[29,30] This might be related to the intrinsic isotropic crystal growth behavior of Pt, which appears quite different from that of other noble metals such as Au and Ag.[31−33] As a result, the number of reports on the direct synthesis of high-aspect-ratio Pt nanorods/nanowires is very limited in the literature.[34] Furthermore, the assembly or oriented arrangement of ultrathin noble-metal nanowires is expected to play an important role in the fabrication of future nanoscale devices.[35−39] For example, Pt nanowire arrays have been reported to serve as potential interconnect platforms,[40] high-frequency nanomechanical resonators,[41] and surface plasmon resonators;[42] also Pt nanowire films have been used as transparent electrodes and transistors.[43] The oriented arrangement or assembly of metal nanowires normally involves the introduction of templates, substrates, or even external electric or magnetic fields.[44−47]

Herein we report a one-pot synthesis of ultrathin (~3 nm) and ultralong (~10 μm) Pt nanowires and their spontaneous self-assembly into bundles (20–30 nm in diameter), without the use of any stabilizer, template, or external field (see the Supporting Information for the experimental details). This solvothermal method is facile, highly reproducible, and easy to scale up. To the best of our knowledge, there has been no report of the direct preparation of such ultrathin Pt nanowire assemblies in solution. An oriented attachment mechanism for Pt nanowire assembly formation is proposed in which amine species plays a key role in the formation of the ultralong and ultrathin Pt nanowires. Importantly, it is also demonstrated that this strategy can be applied to the preparation of other alloyed noble-metal nanowire assemblies (e.g., Pt–Au, Pt–Pd). Furthermore, a free-standing two-dimensional (2D) nanowire

Received: March 24, 2013
Published: June 6, 2013

   dx.doi.org/10.1021/ja402955t | J. Am. Chem. Soc. 2013, 135, 9480–9485

membrane has been fabricated from these nanowire assemblies. The as-prepared nanowire membrane exhibits excellent electrocatalytic activity and superior stability toward the oxidation of small fuel molecules such as methanol and formic acid and the oxygen reduction reaction (ORR).

EXPERIMENTAL SECTION

Preparation of Pt Nanowire Assemblies. In a typical synthesis, 100 mg of H_2PtCl_6 solution (8 wt %) and 500 mg of potassium hydroxide (KOH) were added to a mixed solution containing 4 mL of ethylene glycol (EG) and 6 mL of *N*,*N*-dimethylmethanamide (DMF). After magnetic stirring for 12 h, the resultant homogeneous and transparent solution was transferred into a 25 mL Teflon-lined autoclave. The autoclave was maintained at 170 °C for 8 h and then cooled to room temperature. The black products were collected and washed with ethanol and DI water several times before drying at 80 °C overnight. Pt-based Pt−Au and Pt−Pd alloy nanowire assemblies were also prepared by the same method with the addition of Au and Pd precursors with different metal ratios. The mass yield of Pt nanowire assemblies is about 90%.

Fabrication of Free-Standing Pt Nanowire Membrane. A free-standing Pt nanowire membrane was fabricated by a solvent evaporation induced self-assembly process. Briefly, Pt nanowire assemblies were dispersed in ethanol with vigorous ultrasonication for 2 h to form a black homogeneous suspension. A certain volume of the suspension was then poured into a Teflon container. The solvent was allowed to evaporate slowly at room temperature for 48 h, and the free-standing Pt nanowire membrane was obtained.

Materials Characterization. Powder X-ray diffraction (XRD) patterns were recorded using a Bruker diffractometer with Cu Kα radiation (D8 Advance X-ray diffractometer, Cu Kα, λ = 1.5406 Å, 40 kV, and 40 mA) to study the crystallographic information of the samples. Field-emission scanning electron microscopy (FESEM; JEOL, JSM-6700F, 5 kV) equipped with energy-dispersive X-ray spectroscopy (EDX) was used to analyze the morphology and elemental composition of the samples. The morphology and microstructure of the products were further studied by transmission electron microscopy (TEM; JEOL, JEM-2010, 200 kV) and high-resolution transmission electron microscopy (HRTEM; JEOL, JEM-2100F, 200 kV). Selected-area electron diffraction (SAED) was performed to study the crystallinity and structure of the samples. Thermogravimetric analysis (TGA) was carried out under a flow of air with a temperature ramp of 10 °C min^{-1} from room temperature to 600 °C. The Fourier-transform infrared spectroscopy (FT-IR) spectra were recorded from KBr disks using a Perkin-Elmer GX instrument in the wavenumber range of 4000−400 cm^{-1}. The surface properties of the samples were analyzed with X-ray photoelectron spectroscopy (XPS; VG ESCALAB MKII instrument) that uses a Mg Kα X-ray source. The survey scans were collected by using a pass energy of 160 eV. High-resolution spectra of the individual elements were collected with the analyzer pass energy set at 40 eV. The pressure of the analyzer chamber was maintained at 10^{-9} Pa during the measurement. Before the analysis, all the samples were dried under vacuum at 80 °C overnight.

Electrochemical Measurements. The electrochemical activity of the Pt nanowire assemblies and commercial Pt/C (Johnson Matthey, 20 wt %) electrocatalysts was characterized by the cyclic voltammetry (CV) technique. The experiment was performed using a three-electrode cell with an Autolab potentiostat/galvanostat (Model PGSTAT-72637) workstation at ambient temperature. A glassy-carbon (GC)-disk electrode (5 mm in diameter) served as the substrate for the support. Prior to use, the GC electrode was polished using an aqueous alumina suspension on felt polishing pads. A round as-prepared Pt nanowire membrane (~4 mm in diameter, 42 ug) was adhered on the GC-disk electrode using Nafion solution (10 uL, 0.5 wt %). For comparison, the Pt/C catalyst dispersion was prepared by mixing 8 mg of catalyst in 2.5 mL of solution containing 2.4 mL of ethanol and 100 μL of 0.5 wt % Nafion solution followed by 30 min of ultrasonication. Then the Pt/C catalyst suspension was pipetted by micropipettor on the GC surface, leading to a Pt loading of about 0.2 mg cm^{-2}. The working electrode was dried under an N_2 flow at room temperature. A saturated calomel electrode (SCE) and a large-area Pt plate were used as the reference and counter electrodes, respectively. The CV profiles were recorded at a scan rate of 20 mV s^{-1} within the potential range from −0.241 to 1 V vs SCE in a 0.5 M H_2SO_4 solution. Formic acid and methanol oxidation measurements were carried out with a scan rate of 20 mV s^{-1} in a solution containing 0.5 M H_2SO_4 + 0.5 M CH_3OH and 0.5 M H_2SO_4 + 0.5 M HCOOH, respectively. The CO stripping experiments for Pt nanowire assemblies and commercial PtRu/C (33.3%) and Pt/C electrocatalysts were conducted following the procedure below. N_2 was bubbled into a 0.5 M H_2SO_4 solution for 30 min, and then the solution was bubbled by CO for 40 min while keeping the potential at −0.14 V vs SCE for CO poisoning, and then the solution was bubbled by N_2 vigorously to remove the dissolved CO. CV profiles were recorded at a scan rate of 20 mV s^{-1}. The ORR measurements were performed in an oxygen-saturated H_2SO_4 solution (0.5 M) at room temperature with a sweep rate of 10 mV s^{-1}. The ORR pathway was measured by rotating ring-disk electrode (RRDE) measurements with a bipotentiostat (Autolab) and rotation control (Pine Instruments). The Pt-ring electrode was potentiotated at 1.1 V (vs RHE), where the detection of peroxide is diffusion limited. Before the RRDE tests, the collection efficiency (N) was determined from the ring (I_R) and disk (I_D) currents, $N = -I_R/I_D$, which are obtained in 0.1 M NaOH electrolyte supplemented with 10 mM $K_3Fe(CN)_6$ at a sweep rate of 20 mV s^{-1} (ring potential at 1.1 V vs RHE). For convenience, all potentials in ORR tests are referenced to the reversible hydrogen electrode (RHE). For long-term stability tests, accelerated CV tests were also conducted for 3000 cycles.

RESULTS AND DISCUSSION

In a typical synthesis of Pt nanowire assemblies, chloroplatinic acid hexahydrate ($H_2PtCl_6{\cdot}6H_2O$) and potassium hydroxide (KOH) were dissolved in a mixed solvent of *N*,*N*-dimethylmethanamide (DMF) and ethylene glycol (EG). After magnetic stirring for 12 h, the resultant homogeneous and transparent solution was then solvothermally treated in a Teflon-lined stainless steel autoclave (25 mL in capacity) at 170 °C for 8 h. Figure 1a shows a representative field-emission scanning electron microscopy (FESEM) image of Pt nanowire assemblies with a diameter of about 30 nm. The assemblies are very flexible and have a length up to 10 μm. By simple casting of the Pt nanowire suspension on a Teflon substrate, a Pt nanowire membrane can be obtained after drying naturally at ambient temperature. The paperlike Pt membrane is flexible and can be easily detached from the substrate without damage (inset of Figure 1a). Energy dispersive X-ray (EDX) analysis (Figure S1, see the Supporting Information) and X-ray diffraction (XRD; Figure S2, see the Supporting Information) results confirm that the as-prepared samples consist exclusively of Pt with a face-centered cubic (fcc) structure (JCPDS No. 04-0802). The morphology and structure of the Pt nanowire assemblies have been further characterized by transmission electron microscopy (TEM). An overview TEM image of the product displays a network structure composed of interconnected ultralong Pt nanowires (Figure 1b), consistent with the FESEM observation. Interestingly, the high-magnification TEM image (inset of Figure 1b) reveals that these Pt wires consist of aligned ultrathin Pt nanowires about 3 nm in diameter. A small amount of individual nanowires or binanowires can also be observed. High-resolution (HR) TEM images of these individual nanowires show clear lattice fringes with an interplanar distance of approximately 0.227 nm, corresponding to Pt(111) planes (Figure 1c,d). The selected-area electron diffraction (SAED) pattern (inset of Figure 1c) corresponding to Figure 1c indicates the high crystallinity of these single-

dx.doi.org/10.1021/ja402955t | J. Am. Chem. Soc. 2013, 135, 9480−9485

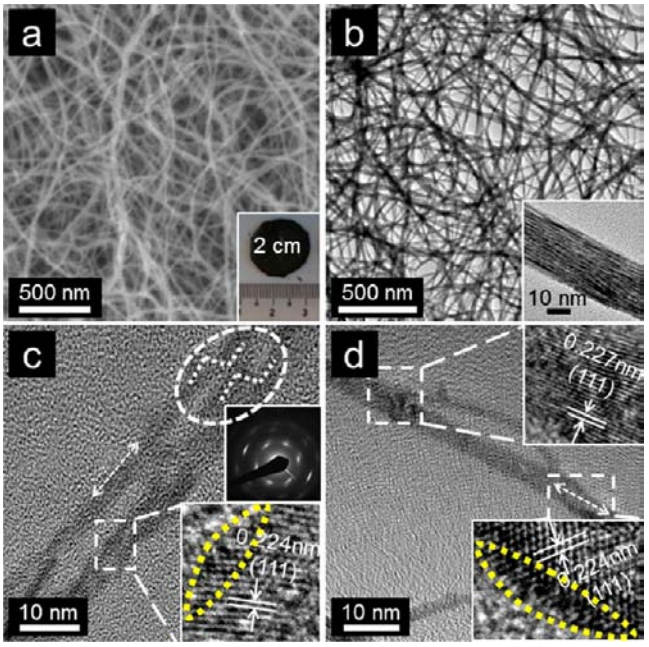

Figure 1. (a) FESEM, (b) TEM, and (c, d) HRTEM images of Pt nanowire assemblies. The inset in (a) shows an optical photo of a Pt nanowire membrane, 2 cm in diameter, fabricated by a simple casting process. The insets in (b)−(d) show the corresponding high-magnification images. One inset in (c) displays the SAED pattern. The mismatch of Pt nanowires is indicated by the white circle in (c). The surface atomic arrangements of nanowires are also shown in the insets of (c) and (d), which indicate the existence of step structures on the surface of Pt nanowires. The double arrows in (c) and (d) indicate the ⟨111⟩ growth direction of Pt nanowires.

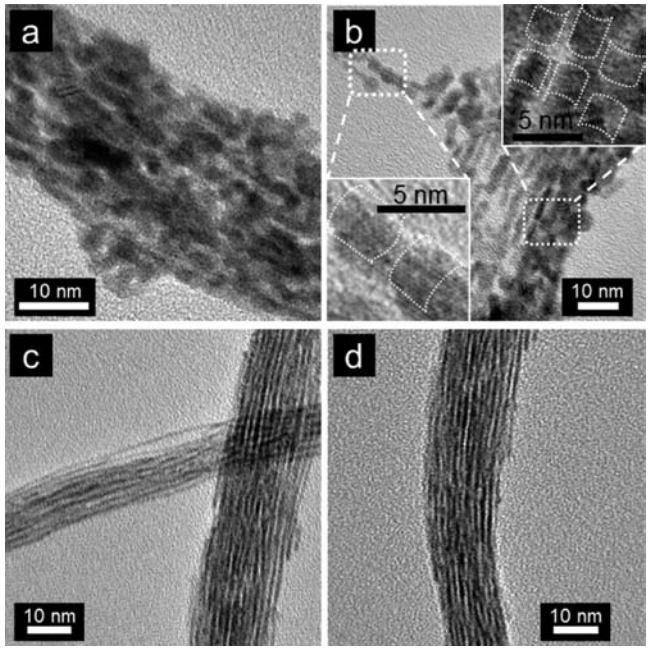

Figure 2. TEM images of the products obtained with different reaction durations: (a) 1 h; (b) 2 h; (c) 5 h; (d) 12 h. The insets in (b) are high-magnification TEM images.

crystal Pt nanowires. Interestingly, the as-prepared nanowires grow along the ⟨111⟩ direction and possess abundant step structure and high index exposed facets, as shown in Figure 1c,d.

To better understand the formation process and growth mechanism of these unusual Pt nanowire assemblies, the intermediate products collected at different reaction durations were investigated by TEM. Figure 2 shows the morphological and structural evolution of Pt nanowire assemblies with the reaction time. Figure 2a reveals that the product collected after reaction for 1 h mainly exists as a directed 1D alignment of nanoparticles. These 1D aligned nanoparticles are further assembled side by side in parallel, as shown in Figure 2b. With an increase in reaction time, coalescence of nanoparticles in the aligned direction occurred to form nanorods and eventually nanowires, while different nanowires assembled together without coalescence among them. After reaction for 5 h, the Pt nanowire assemblies were formed (Figure 2c), and no further pronounced change in the Pt nanowire assemblies was observed even though the reaction time was prolonged to 12 h (Figure 2d). Therefore, the presence of Pt nanoparticle chains and subsequent rearrangement along the preferred crystallographic axis suggest that the nanowires obtained in this work are formed not through a seed-initiated growth process[48] but rather by the oriented alignment and attachment mechanism.[49,50] Meanwhile, fusion and recrystallization and even rearrangement and reconstruction of the Pt nanocrystals facing each other would also occur, as shown in the insets of Figure 2b, leading to the formation of nanowires.[51] As can be seen in the circled area in Figure 1c, the presence of a mismatched joint region between parallel nanowires indicates that the nanoparticles or nanorods might be connected via the subsequent growth of Pt from the solution.

It is also found that the amount of KOH in the reaction solution plays a very important role in the formation of Pt nanowire assemblies. In the absence of KOH, only Pt nanoparticles were obtained (Figure S3, see the Supporting Information). With the addition of an increasing amount of KOH from 50 to 900 mg, Pt nanowire bundles decorated with nanoparticles were first obtained, then the fraction of nanoparticles was gradually reduced, and finally the nanowire assemblies dominated in the product (Figures S4 and S5, see the Supporting Information). Since no surfactant was added in the initial reaction solution, we propose that the amine species produced from the reaction of DMF and KOH would be adsorbed on Pt nanostructures and affect the formation of Pt nanowire assemblies. The presence of amine molecules in the purified nanowire assemblies is indicated by the weight loss from the thermogravimetric analysis (TGA; Figure S6a, see the Supporting Information). The Fourier transform infrared spectroscopy (FT-IR) result also confirms the presence of amine groups (Figure S6b, see the Supporting Information). X-ray photoelectron spectroscopy (XPS) was employed to analyze the elements, and the presence of N and C species was further revealed in the as-prepared samples. Moreover, Pt nanowire assemblies exhibited a higher percentage amount (~62%) of Pt(0) species than the commercial Pt/C catalyst (~42%). This would be beneficial for improving the catalytic activity, because the oxide species on the Pt surface is largely inactive (Figures S7 and S8, see the Supporting Information). It has been reported that oleylamine, with a long chain, can serve as the stabilizer and structure-directing agent for the formation of nanowires and branched nanocrystal assemblies.[52] In the present system, with an increasing amount of KOH, more amine species would be generated in the reaction solution. These small amine molecules would guide the growth of

dx.doi.org/10.1021/ja402955t | J. Am. Chem. Soc. 2013, 135, 9480−9485

nanowires in one dimension, and the simultaneous self-assembly of Pt nanowires to form Pt bundles may be simply driven by the reduction of total surface energy.[47] The adsorption of these small amine molecules may also explain the presence of small inter-nanowire space between Pt nanowires in the assembly. Similar Pt nanowire assemblies can be obtained by replacing KOH with NaOH, as shown in Figure 3a (also in Figure S9, see the Supporting Information).

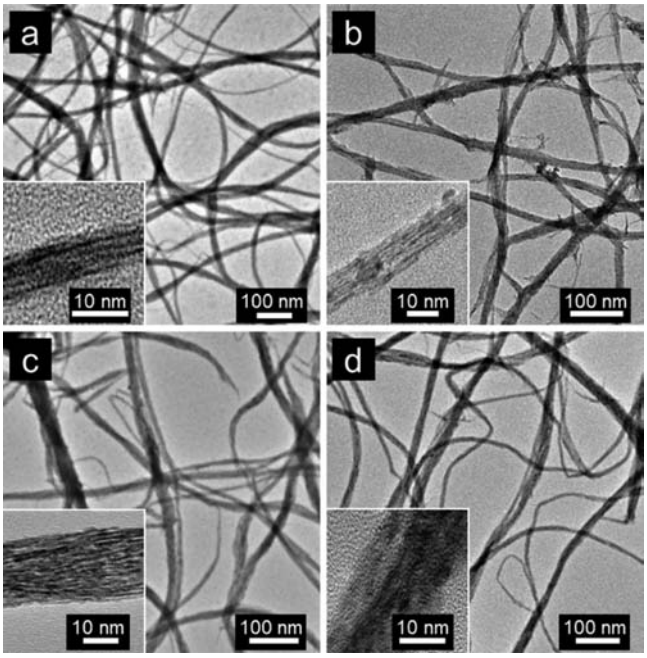

Figure 3. TEM images of Pt nanowire assemblies obtained by (a) replacing KOH with NaOH, (b) replacing EG with H_2O, and (c) Pt–Au and (d) Pt–Pd alloy nanowire assemblies. The corresponding high-magnification TEM images are shown in the insets.

It is known that KOH cannot dissolve in DMF under ambient conditions. In this study, EG was therefore used as the cosolvent to dissolve KOH. With the addition of EG, a homogeneous and transparent solution can be formed (Figure S10, see the Supporting Information). In the mixed solvent with different EG/DMF volume ratios, a Pt nanowire assembly can be obtained after a solvothermal reaction (Figure S11, see the Supporting Information). As shown in Figure 3b, similar Pt nanowire assemblies can also be obtained by replacing EG with H_2O as long as the content of H_2O in the mixed H_2O/DMF solvent is not dominant (Figure S12, see the Supporting Information). Remarkably, the current approach can be easily extended to the formation of nanowire assemblies of other Pt-based alloys such as Pt–Pd and Pt–Au (Figure 3c,d) with different atomic ratios (Figure S13, see the Supporting Information). The Pt–Au and Pt–Pd nanowire assemblies exhibit the solid solution structure from the TEM and HRTEM observations (Figure S14, see the Supporting Information), also confirmed by XRD patterns (Figure S15, see the Supporting Information).

Recently, membranes made of Pt nanostructures have attracted great interest because of the many novel structural characteristics and unique properties of the interwire assembly, such as high porosity, good flexibility, large area per unit volume, and interconnected open pore structures.[47,49] Therefore, a membrane made of the present Pt nanowire assemblies would be a promising electrode catalyst in view of the large surface area of about 90 $m^2\ g^{-1}$ and high porosity (Figure S16, see the Supporting Information). The electrocatalytic performance of a Pt nanowire assembled membrane was evaluated in a 0.5 M H_2SO_4 solution with a sweep rate of 20 mV s^{-1} at room temperature. For comparison, a commercial carbon-supported Pt (Pt/C) electrocatalyst (Johnson Matthey, JM 20 wt %) was also evaluated under identical conditions. Figure 4a,b shows

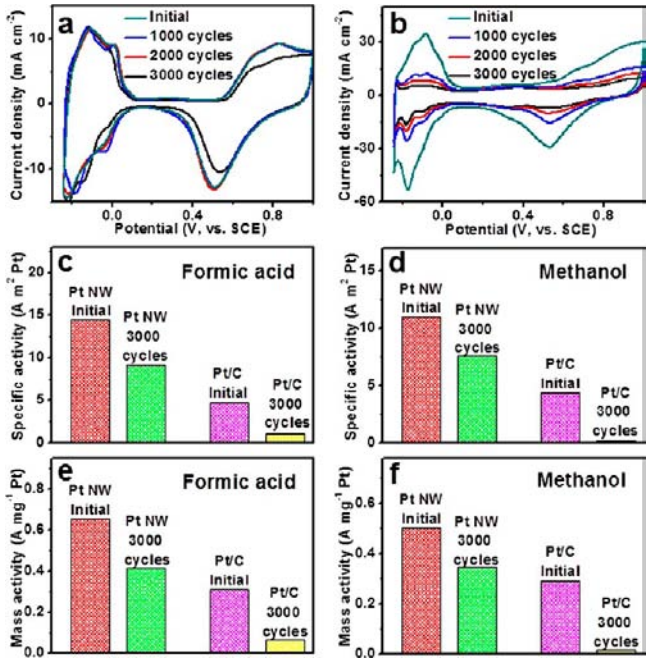

Figure 4. Electrochemical evaluation. Cyclic voltammetry (CV) curves of Pt nanowire membrane (a) and the commercial Pt/C electrocatalyst (b) before and after 1000–3000 cycles of accelerated stability tests. CV curves were recorded in a 0.5 M H_2SO_4 solution with a scan rate of 20 mV s^{-1}. Comparative specific (c, d) and mass (e, f) activity for formic acid (c, e) and methanol oxidation (d, f) before and after 3000 cycles of Pt nanowire (NW) membrane and commercial Pt/C electrocatalyst.

cyclic voltammetry (CV) curves of the Pt nanowire membrane and the commercial Pt/C electrocatalyst, respectively, both before and after cycling for up to 3000 cycles. In comparison with the commercial Pt/C catalyst, the Pt nanowire membrane exhibits distinct hydrogen adsorption–desorption peaks, suggesting the existence of better ordered surface structures (insets of Figure 1c,d).[53] The electrochemical active surface area (ECSA) of Pt electrocatalysts can be estimated by integrating the charge passed during the hydrogen adsorption–desorption from the electrode surface after the double-layer correction.[53] The ECSA value obtained for the Pt nanowire membrane is 45.6 $m^2\ g^{-1}$, which is about 70% of that of the commercial Pt/C electrocatalyst (65.2 $m^2\ g^{-1}$). The low ECSA for the Pt nanowire catalyst is perhaps due to the assembly of Pt nanowires and residual impurity adsorbed on the surface of Pt nanowires. After 1000 and 3000 accelerated cycles, the commercial Pt/C electrocatalyst loses 75% and 93% of the initial ECSA (Figure 4b), respectively, caused by Pt nanoparticle ripening and aggregation due to carbon corrosion.[54] In a vast contrast, the Pt nanowire membrane only loses 5% and 10% of its initial ECSA after 1000 and 3000 cycles (Figure 4a), respectively. The above results evidently

dx.doi.org/10.1021/ja402955t | J. Am. Chem. Soc. 2013, 135, 9480–9485

show that the Pt nanowire membrane is much more stable than the commercial Pt/C electrocatalyst, thanks to the structural advantages of the former. We have also investigated the electrocatalytic oxidation of small fuel molecules (methanol and formic acid) on the Pt nanowire membrane and commercial Pt/C electrocatalyst (Figure S17, see the Supporting Information). In the initial cycle, the specific electrocatalytic activity of the Pt nanowire membrane is about 3.04 and 2.48 times that of the commercial Pt/C electrocatalyst for formic acid and methanol oxidation, respectively (Figure 4c,d). The mass activity for the Pt nanowire membrane is also 2.13 and 1.74 times that of the commercial Pt/C electrocatalyst for formic acid and methanol oxidation, respectively (Figure 4e,f). The enhanced electrocatalytic performance of the Pt nanowire membrane could be ascribed to the unique free-standing structures built from ultralong and ultrathin Pt nanowires.[12,53] Specifically, the anisotropic interconnected nanowires can improve electron transport and catalyst utilization; meanwhile, the unique network structure of the nanowire membrane can facilitate mass exchange and gas diffusion during the electrochemical reaction. After 3000 cycles, the Pt nanowire membrane shows only about 37% and 31% loss of the activity for formic acid and methanol oxidation, respectively. However, the commercial Pt/C electrocatalyst has degraded considerably: about 79% and 95% for formic acid and methanol oxidation, respectively. The CO-stripping measurements also confirmed that the Pt nanowire assembly has enhanced electrochemical stability in comparison to the commercial PtRu and Pt/C catalysts (Figure S18, see the Supporting Information). We have also evaluated the electrocatalytic activity of the Pt nanowire assembly and commercial Pt/C catalysts toward the ORR before and after 3000 cycles (which takes about 21 h), as shown in Figure S19 (see the Supporting Information). The number of electrons calculated from the slope is about 3.8 for the Pt nanowire assembly, indicating a four-electron process (Figure S19b, see the Supporting Information). The collection efficiency on an RRDE in 0.1 M NaOH electrolyte supplemented with 10 mM $K_3Fe(CN)_6$ is 0.25 ± 5% (Figure S20, see the Supporting Information). The RRDE results also confirm that the ORR proceeds almost entirely through a direct four-electron pathway which is similar to that for the commercial Pt/C catalyst (Figure S21, see Supporting Information).

More importantly, the half-wave potential shift of the Pt nanowire assembly after the long-term durability test is smaller than that of commercial Pt/C catalysts. This clearly indicates that the Pt nanowire assembly has enhanced electrochemical stability in comparison to the commercial Pt/C catalyst. From the above measurements, this free-standing Pt nanowire membrane electrocatalyst exhibits excellent activity and remarkably high stability, making it promising for practical use in low-temperature fuel cells.

CONCLUSIONS

In summary, ultrathin (~3 nm) Pt nanowires with length up to 10 μm have been directly prepared by a facile solvothermal method. These ultrathin Pt nanowires self-assemble into bundles with a diameter of about 30 nm. It is revealed that the oriented attachment mechanism is partially responsible for the formation of these unique Pt nanowires. The amine groups generated from the solvent during the reaction are found to play an important role in the self-assembly of Pt nanowires. This method has also been successfully extended to synthesize other Pt-based alloy (e.g., Pt−Au and Pt−Pd) nanowire assemblies. When it is evaluated as an electrocatalyst, the free-standing membrane fabricated from these self-assembled Pt nanowires manifests high electrocatalytic activity and significantly improved long-term stability in comparison to one commercial Pt/C electrocatalyst. The excellent electrocatalytic performance of the as-made Pt nanowire membrane might be mainly ascribed to the unique structural features of 1D anisotropic nanowire building blocks with high stability and crystallinity and the derived interconnected network with high surface area and large porosity.

ASSOCIATED CONTENT

Supporting Information

Figures giving more data from FESEM/EDX, TEM, XRD, BET, TGA, FTIR, and XPS characterizations and electrochemical measurements. This material is available free of charge via the Internet at http://pubs.acs.org.

AUTHOR INFORMATION

Corresponding Author

*X.W.: e-mail, wangxin@ntu.edu.sg. X.W.L.: e-mail, xwlou@ntu.edu.sg; homepage, http://www.ntu.edu.sg/home/xwlou/.

Notes

The authors declare no competing financial interest.

ACKNOWLEDGMENTS

We are grateful to the Ministry of Education (Singapore) for the academic research fund ARC 2/10 (MOE2009-T2-2-024) and the National Research Foundation (Singapore) for the Competitive Research Program (2009 NRF-CRP 001-032).

REFERENCES

(1) Bezryadin, A.; Lau, C. N.; Tinkham, M. *Nature* **2000**, *404*, 971.
(2) Xia, Y. N.; Yang, P. D.; Sun, Y. G.; Wu, Y. Y.; Mayers, B.; Gates, B.; Yin, Y. D.; Kim, F.; Yan, Y. Q. *Adv. Mater.* **2003**, *15*, 353.
(3) Wang, C.; Hu, Y.; Lieber, C. M.; Sun, S. *J. Am. Chem. Soc.* **2008**, *130*, 8902.
(4) Teng, X.; Han, W.-Q.; Ku, W.; Hücker, M. *Angew. Chem., Int. Ed.* **2008**, *47*, 2055.
(5) Cademartiri, L.; Ozin, G. A. *Adv. Mater.* **2009**, *21*, 1013.
(6) Lu, Y.; Huang, J. Y.; Wang, C.; Sun, S. H.; Lou, J. *Nat. Nanotechnol.* **2010**, *5*, 218.
(7) Guo, S. J.; Li, D. G.; Zhu, H. Y.; Zhang, S.; Markovic, N. M.; Stamenkovic, V. R.; Sun, S. H. *Angew. Chem., Int. Ed.* **2013**, *52*, 3465.
(8) Fu, X. Y.; Wang, Y.; Wu, N. Z.; Gui, L. L.; Tang, Y. Q. *J. Mater. Chem.* **2003**, *13*, 1192.
(9) Chen, J. Y.; Herricks, T.; Geissler, M.; Xia, Y. N. *J. Am. Chem. Soc.* **2004**, *126*, 10854.
(10) Chen, J. Y.; Xiong, Y. J.; Yin, Y. D.; Xia, Y. N. *Small* **2006**, *2*, 1340.
(11) Tiano, A. L.; Koenigsmann, C.; Santulli, A. C.; Wong, S. S. *Chem. Commun.* **2010**, *46*, 8093.
(12) Koenigsmann, C.; Zhou, W. P.; Adzic, R. R.; Sutter, E.; Wong, S. S. *Nano Lett.* **2010**, *10*, 2806.
(13) Guo, S. J.; Zhang, S.; Sun, X. L.; Sun, S. H. *J. Am. Chem. Soc.* **2011**, *133*, 15354.
(14) Mbindyo, J. K. N.; Mallouk, T. E.; Mattzela, J. B.; Kratochvilova, I.; Razavi, B.; Jackson, T. N.; Mayer, T. S. *J. Am. Chem. Soc.* **2002**, *124*, 4020.
(15) Sun, S. H.; Jaouen, F.; Dodelet, J. P. *Adv. Mater.* **2008**, *20*, 3900.
(16) Liang, H. W.; Liu, S.; Gong, J. Y.; Wang, S. B.; Wang, L.; Yu, S. H. *Adv. Mater.* **2009**, *21*, 1850.
(17) Takai, A.; Yamauchi, Y.; Kuroda, K. *J. Mater. Chem.* **2009**, *19*, 4205.

(18) Liang, H. W.; Liu, S.; Yu, S. H. *Adv. Mater.* **2010**, *22*, 3925.
(19) Sun, S. H.; Zhang, G. X.; Geng, D. S.; Chen, Y. G.; Li, R. Y.; Cai, M.; Sun, X. L. *Angew. Chem., Int. Ed.* **2011**, *50*, 422.
(20) Mbindyo, J. K. N.; Reiss, B. D.; Martin, B. R.; Keating, C. D.; Natan, M. J.; Mallouk, T. E. *Adv. Mater.* **2001**, *13*, 249.
(21) Ford, W. E.; Harnack, O.; Yasuda, A.; Wessels, J. M. *Adv. Mater.* **2001**, *13*, 1793.
(22) Zhang, Z. C.; Hui, J. F.; Liu, Z. C.; Zhang, X.; Zhuang, J.; Wang, X. *Langmuir* **2012**, *28*, 14845.
(23) Kitaura, R.; Nakanishi, R.; Saito, T.; Yoshikawa, H.; Awaga, K.; Shinohara, H. *Angew. Chem.* **2009**, *48*, 8298.
(24) Jung, Y. S.; Lee, J. H.; Lee, J. Y.; Ross, C. A. *Nano Lett.* **2010**, *10*, 3722.
(25) Liu, Z.; Sakamoto, Y.; Ohsuna, T.; Hiraga, K.; Terasaki, O.; Ko, C. H.; Shin, H. J.; Ryoo, R. *Angew. Chem., Int. Ed.* **2000**, *39*, 3107.
(26) Yin, H.; Tang, H.; Wang, D.; Gao, Y.; Tang, Z. *ACS Nano* **2012**, *6*, 8288.
(27) Huo, Z.; Tsung, C.-k.; Huang, W.; Zhang, X.; Yang, P. *Nano Lett.* **2008**, *8*, 2041.
(28) Lu, X.; Yavuz, M. S.; Tuan, H.-Y.; Korgel, B. A.; Xia, Y. *J. Am. Chem. Soc.* **2008**, *130*, 8900.
(29) Lee, E. P.; Peng, Z.; Cate, D. M.; Yang, H.; Campbell, C. T.; Xia, Y. *J. Am. Chem. Soc.* **2007**, *129*, 10634.
(30) Xia, B. Y.; Ng, W. T.; Wu, H. B.; Wang, X.; Lou, X. W. *Angew. Chem., Int. Ed.* **2012**, *51*, 7213.
(31) Pazos-Perez, N.; Baranov, D.; Irsen, S.; Hilgendorff, M.; Liz-Marzan, L. M.; Giersig, M. *Langmuir* **2008**, *24*, 9855.
(32) Kang, Y. J.; Ye, X. C.; Murray, C. B. *Angew. Chem., Int. Ed.* **2010**, *49*, 6156.
(33) Sanchez-Iglesias, A.; Grzelczak, M.; Perez-Juste, J.; Liz-Marzan, L. M. *Angew. Chem., Int. Ed.* **2010**, *49*, 9985.
(34) Wang, C.; Hou, Y. L.; Kim, J. M.; Sun, S. H. *Angew. Chem., Int. Ed.* **2007**, *46*, 6333.
(35) Maier, S. A.; Kik, P. G.; Atwater, H. A.; Meltzer, S.; Harel, E.; Koel, B. E.; Requicha, A. A. G. *Nat. Mater.* **2003**, *2*, 229.
(36) Tseng, R. J.; Tsai, C.; Ma, L.; Ouyang, J.; Ozkan, C. S.; Yang, Y. *Nat. Nanotechnol.* **2006**, *1*, 72.
(37) Zhao, Y.; Thorkelsson, K.; Mastroianni, A. J.; Schilling, T.; Luther, J. M.; Rancatore, B. J.; Matsunaga, K.; Jinnai, H.; Wu, Y.; Poulsen, D.; Frechet, J. M.; Alivisatos, A. P.; Xu, T. *Nat. Mater.* **2009**, *8*, 979.
(38) Nie, Z.; Petukhova, A.; Kumacheva, E. *Nat. Nanotechnol.* **2010**, *5*, 15.
(39) Lai, X.; Halpert, J. E.; Wang, D. *Energy Environ. Sci.* **2012**, *5*, 5604.
(40) Kawasaki, J. K.; Arnold, C. B. *Nano Lett.* **2011**, *11*, 781.
(41) Feng, X. L.; White, C. J.; Hajimiri, A.; Roukes, M. L. *Nat. Nanotechnol.* **2008**, *3*, 342.
(42) Li, M.; Bhiladvala, R. B.; Morrow, T. J.; Sioss, J. A.; Lew, K. K.; Redwing, J. M.; Keating, C. D.; Mayer, T. S. *Nat. Nanotechnol.* **2008**, *3*, 88.
(43) Haussmann, A.; Milde, P.; Erler, C.; Eng, L. M. *Nano Lett.* **2009**, *9*, 763.
(44) Smogunov, A.; Dal Corso, A.; Delin, A.; Weht, R.; Tosatti, E. *Nat. Nanotechnol.* **2008**, *3*, 22.
(45) Min, Y.; Akbulut, M.; Kristiansen, K.; Golan, Y.; Israelachvili, J. *Nat. Mater.* **2008**, *7*, 527.
(46) Shui, J. L.; Li, J. C. M. *Nano Lett.* **2009**, *9*, 1307.
(47) Liu, J. W.; Liang, H. W.; Yu, S. H. *Chem. Rev.* **2012**, *112*, 4770.
(48) Azulai, D.; Cohen, E.; Markovich, G. *Nano Lett.* **2012**, *12*, 5552.
(49) Tang, Z. Y.; Kotov, N. A. *Adv. Mater.* **2005**, *17*, 951.
(50) Li, D.; Nielsen, M. H.; Lee, J. R.; Frandsen, C.; Banfield, J. F.; De Yoreo, J. J. *Science* **2012**, *336*, 1014.
(51) Liao, H. G.; Cui, L.; Whitelam, S.; Zheng, H. *Science* **2012**, *336*, 1011.
(52) Mourdikoudis, S.; Liz-Marzán, L. *Chem. Mater.* **2013**, *25*, 1465.
(53) Liang, H. W.; Cao, X. A.; Zhou, F.; Cui, C. H.; Zhang, W. J.; Yu, S. H. *Adv. Mater.* **2011**, *23*, 1467.
(54) Chen, Z.; Waje, M.; Li, W.; Yan, Y. *Angew. Chem., Int. Ed.* **2007**, *46*, 4060.